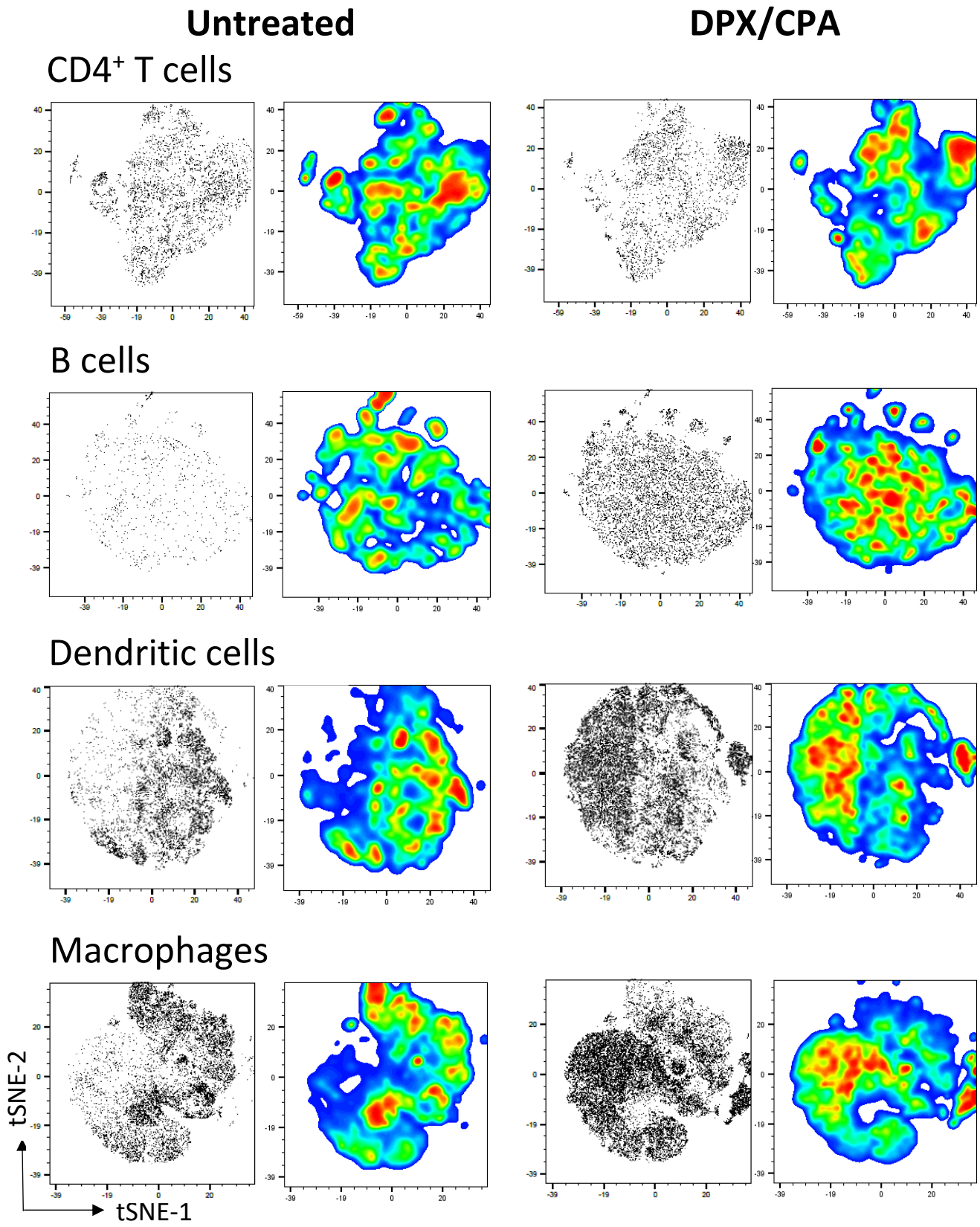
Untreated
DPX/CPA
CD4+ T cells
B cells
Dendritic cells
Macrophages
tSNE-2
tSNE-1

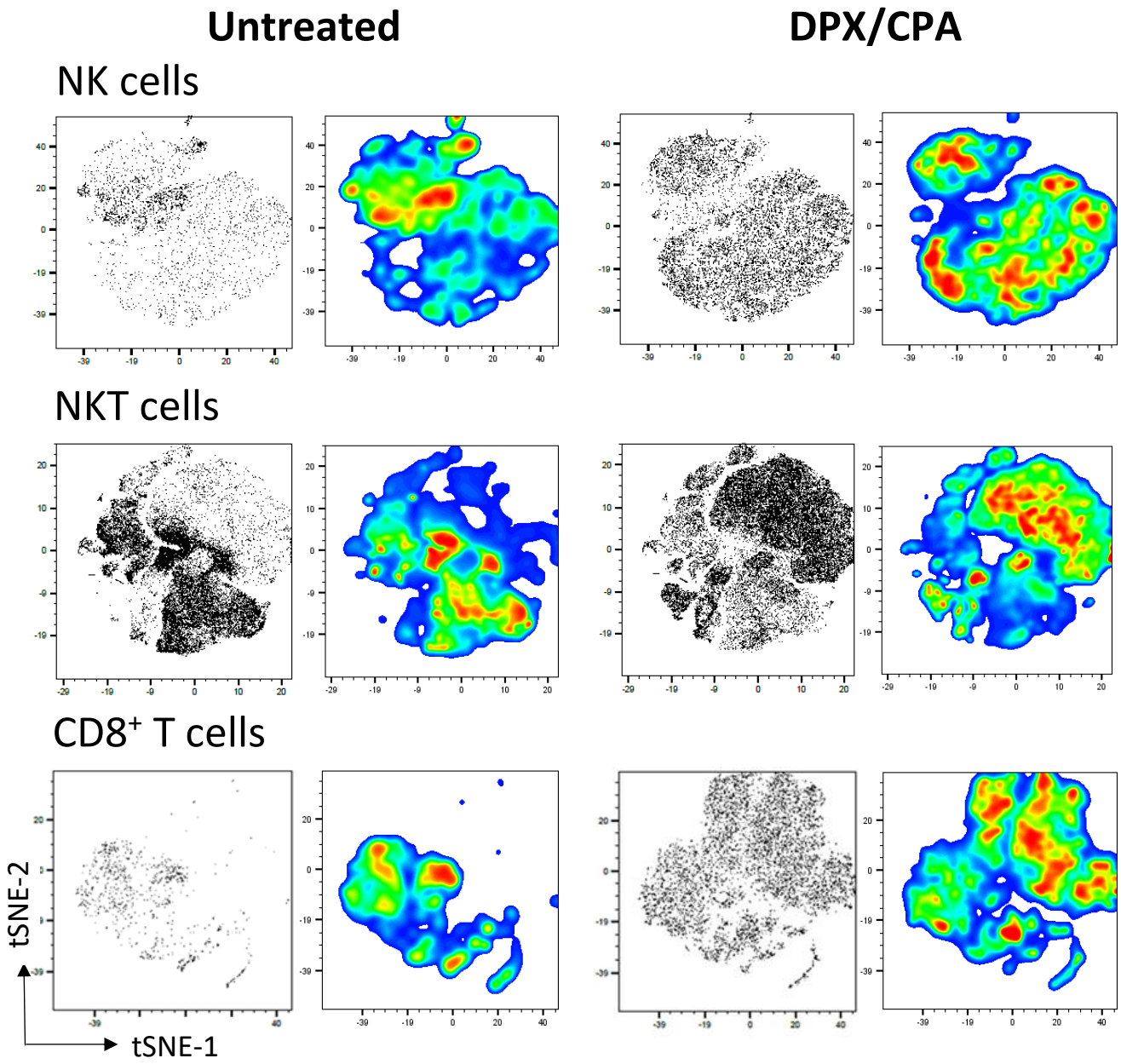

Supplementary Figure 1: Representative tSNE plots of tumor infiltrating cells in C3 tumor. Mice bearing C3 tumors were treated with CPA and DPX-FP. Ten days post DPX-FP treatment, mice were terminated. Tumors were dissociated and analyzed by flow cytometry, using tSNE analysis to determine alterations in populations of tumor infiltrating cells within the tumor. Data presented as dot plots and heat maps for each condition. Markers analyzed by tSNE were CTLA-4, PD-1, OX40, GITR, TIM-3, LAG-3, CD27, CD40, CD137, ICOS, and VISTA. Representative tSNE plots of untreated and treated tumors for the indicated immune cells are shown.

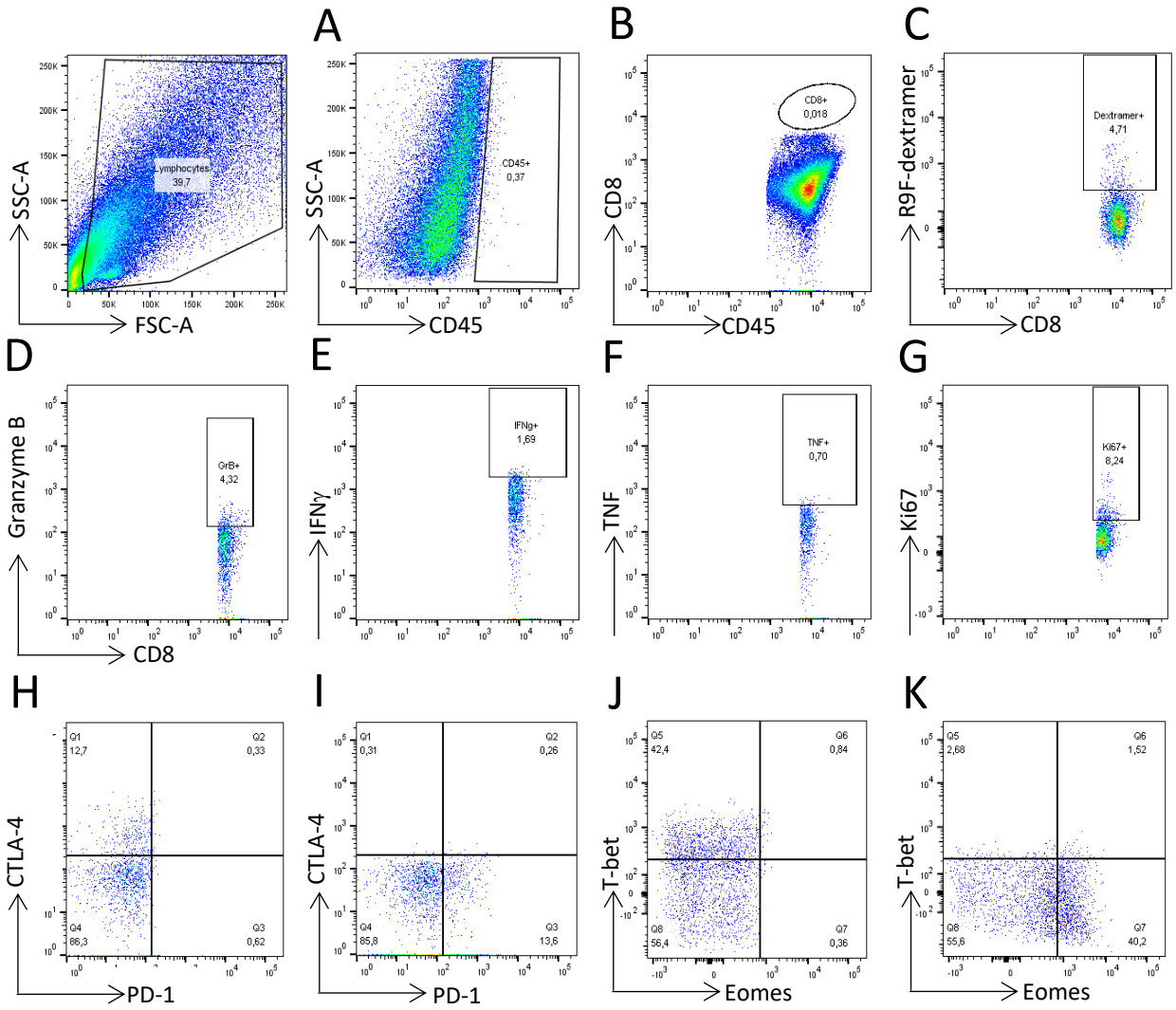

Supplementary Figure 2: Representative Fluorescence Minus One (FMO) control strategy to define regions for the characterization of CD8$^+$T cells recruited to tumor in response to DPX/CPA regimen. Cells were gated based on forward and side scatter thresholds and then gated based on FMO controls lacking the following antibodies from the antibody cocktail: **A)** CD45; **B)** CD8a; **C)** R9F-dextramer; **D)** Granzyme B; **E)** IFNγ; **F)** TNF; **G)** Ki67; **H)** PD-1; **I)** CTLA-4; **J)** Eomes; **K)** T-bet. The values in the gates and/or quadrant plots represent the spread of fluorescence from the other staining parameters, and/or autofluorescence.

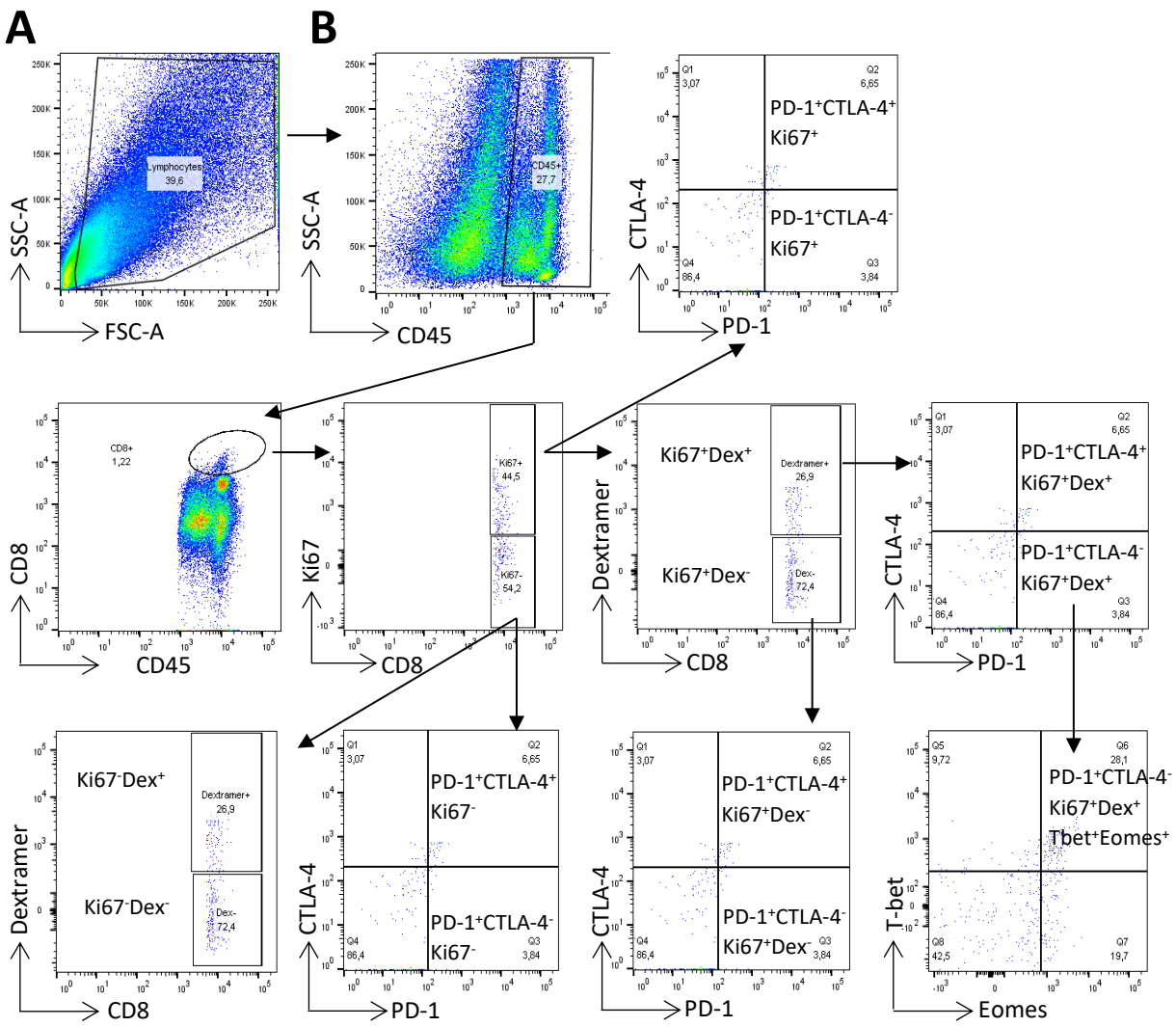

Supplementary Figure 3: Representative analysis of CD8$^+$ T cells recruited to the tumor in untreated mice. Cells were gated based on forward and side scatter thresholds. **A)** Immune cells were then identified through the expression of the CD45 marker. **B)** Gates were set based on FMO controls (Supplementary Figure 2) and unstained cells.

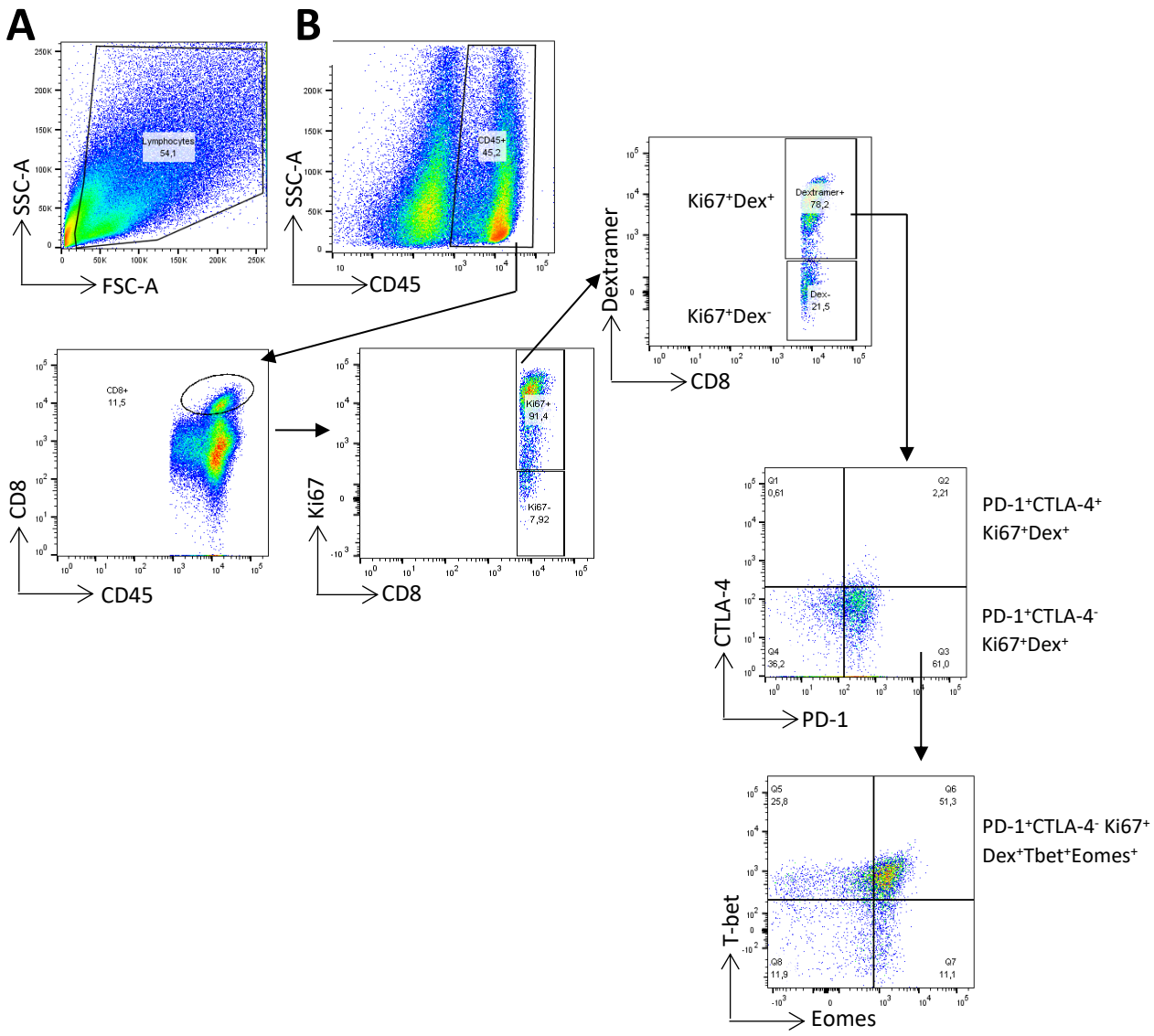

Supplementary Figure 4: Representative analysis of CD8⁺ T cells recruited to the tumor in DPX/CPA-treated mice. A) Cells were gated based on forward and side scatter thresholds. **B)** Immune cells then were identified through the expression of the CD45 marker. Gates were set based on FMO controls (Supplementary Figure 2) and unstained cells.

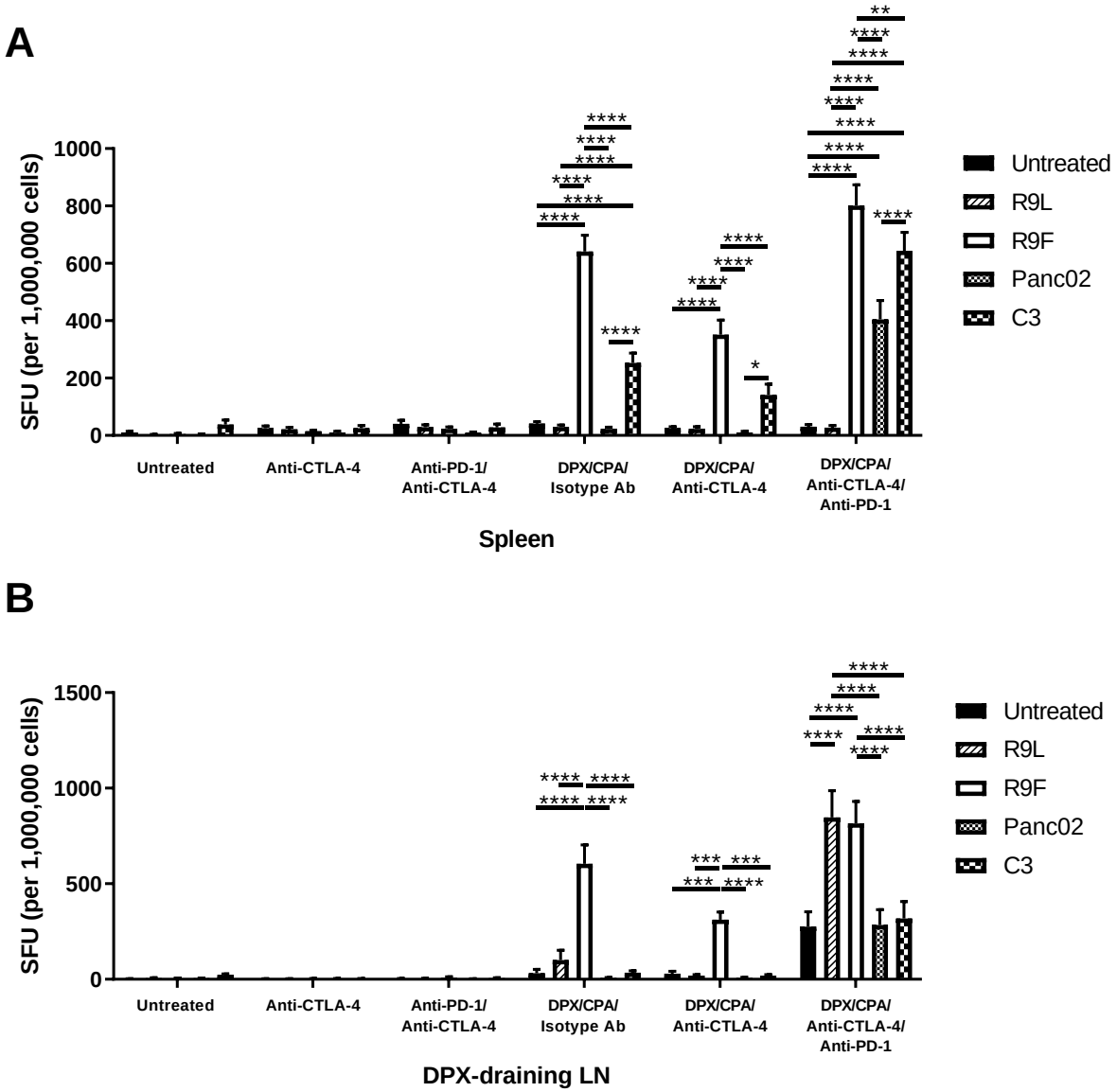

Supplementary Figure 5: Impact of DPX/CPA/CTLA-4 blockade with and without PD-1 blockade on antigen-specific IFN-γ production. Mice bearing C3 tumors were treated with CPA, DPX-FP and isotype antibody (Ab) or anti-CTLA-4 (day of DPX-FP treatment) with or without anti-PD-1 (6 days after DPX-FP treatment). Ten days post DPX-FP treatment, mice were terminated. Spleens and DPX-draining lymph nodes were collected for immune analysis by IFN-γ ELISPOT assay. **A)** Splenocytes either unstimulated (background), or stimulated with irrelevant peptide, irrelevant Panc02 cells, R9F peptide, or C3 cells; **B)** Lymph node cells were stimulated with syngeneic dendritic cells unloaded or loaded with irrelevant peptide or R9F peptide, or irrelevant Panc02 cells or C3 cells. n = 5-8, average ± SEM, statistics by two-way ANOVA, * $p<0.05$, ** $p<0.01$, *** $p<0.001$, **** $p<0.0001$

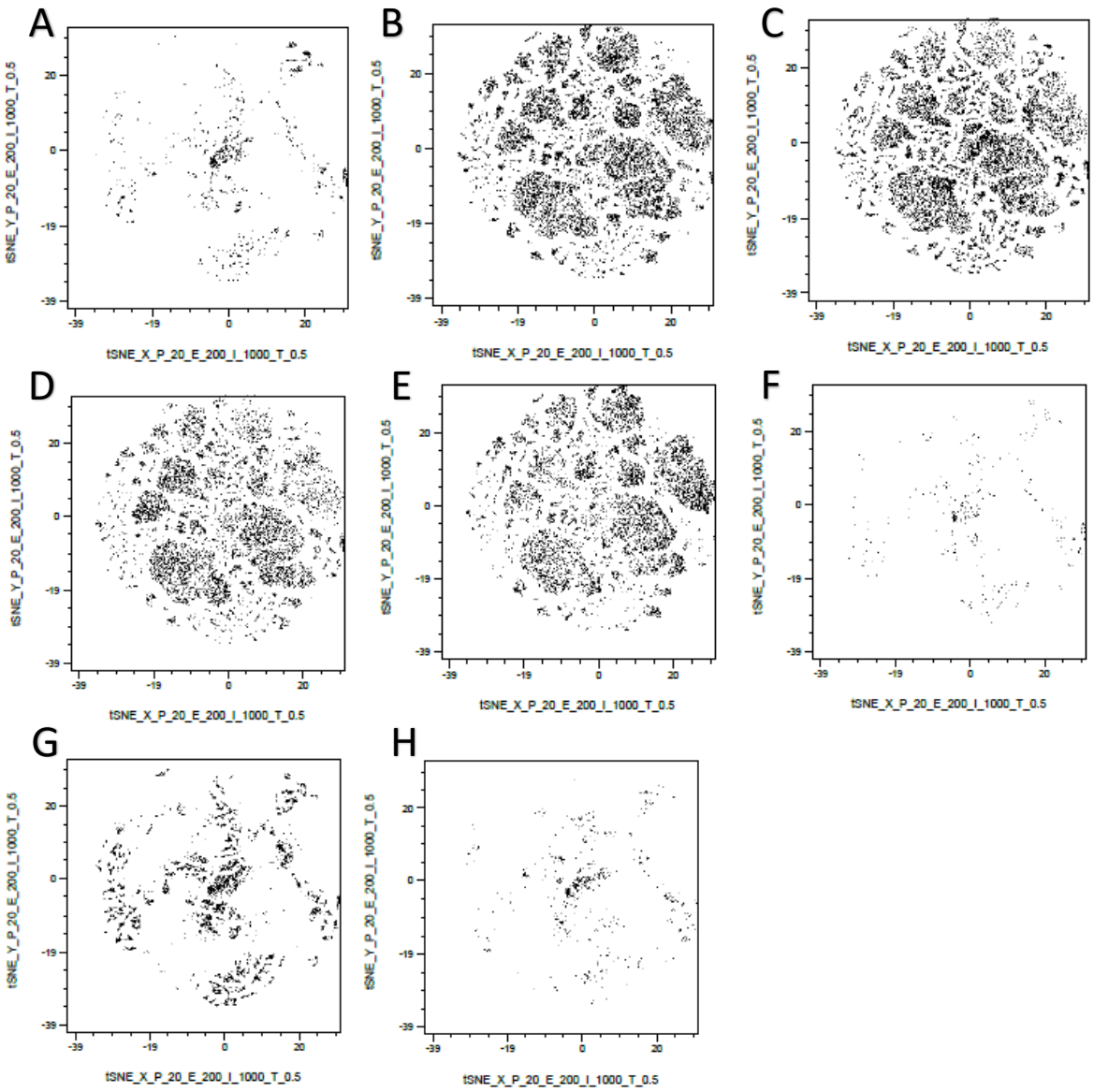

Supplementary Figure 6: Representative tSNE plots of CD8$^+$ T cells in C3 tumor. Mice bearing C3 tumors were treated with CPA, DPX-FP and isotype antibody (Ab) or anti-PD-1 (6 days after DPX-FP treatment) and/or anti-CTLA-4 (day of DPX-FP treatment). Ten days post DPX-FP treatment, mice were terminated. Tumors were dissociated and analyzed by flow cytometry, using tSNE analysis to determine alterations in populations of CD8$^+$ T cells within the tumor. Markers analyzed by tSNE were granzyme B, PD-1, CTLA-4, Eomes, R9F-Dextramer (for peptide-specificity), TNF, Tbet, IFNγ and Ki67 (as a marker of proliferation). Representative tSNE plots of CD8$^+$ T cells from: **A)** untreated, **B)** DPX/CPA/Isotype Ab, **C)** DPX/CPA/anti-PD-1, **D)** DPX/CPA/anti-CTLA-4, **E)** DPX/CPA/anti-CTLA-4/anti-PD-1, **F)** anti-PD-1 alone, **G)** anti-CTLA-4 alone, and **H)** anti-PD-1/anti-CTLA-4.